CRC Report No. A-137

MULTI-SCALE ANALYSIS OF PM SOURCES NEAR HIGHWAYS AND TRANSPORTATION CORRIDORS

Final Report

October 2025

COORDINATING RESEARCH COUNCIL, INC.
1 CONCOURSE PARKWAY • SUITE 800 • ATLANTA, GA 30328

The Coordinating Research Council, Inc. (CRC) is a non-profit corporation supported by the petroleum and automotive equipment industries with participation from other industries, companies, and governmental bodies on research programs of mutual interest. CRC operates through the committees made up of technical experts from industry and government who voluntarily participate. The five main areas of research within CRC are: air pollution (atmospheric and engineering studies); aviation fuels, lubricants, and equipment performance; heavy-duty vehicle fuels, lubricants, and equipment performance (e.g., diesel trucks); light-duty vehicle fuels, lubricants, and equipment performance (e.g., passenger cars); and sustainable mobility (e.g., decarbonization). CRC's function is to provide the mechanism for joint research conducted by industries that will help in determining the optimum combination of products. CRC's work is limited to research that is mutually beneficial to the industries involved. The final results of the research conducted by, or under the auspices of, CRC are available to the public.

Prepared for:

Coordinating Research Council
5755 North Point Parkway, Suite 265
Alpharetta, GA 30022

Prepared by:

Ramboll Americas Engineering Solutions, Inc.
7250 Redwood Blvd., Suite 105
Novato, CA 94945

August 2025
1940111767

CRC PROJECT A-137 DRAFT FINAL REPORT

Multi-scale Analysis of PM Sources Near Highways and Transportation Corridors

CRC PROJECT A-137 DRAFT FINAL REPORT
MULTI-SCALE ANALYSIS OF PM SOURCES NEAR HIGHWAYS AND TRANSPORTATION CORRIDORS

Ramboll
7250 Redwood Boulevard
Suite 105
Novato, CA 94945
USA

T +1 415 899 0700
https://ramboll.com

CONTENTS

Table of Figures

Table of Tables

LIST OF ACRONYMS AND ABBREVIATIONS

3-D	Three-dimensional
AADT	Annual Average Daily Traffic
ACM2	Asymmetric Convective Mixing, version 2
AMET	Atmospheric Model Evaluation Tool
AOD	Aerosol Optical Depth
AQRP	Air Quality Research Program
AQS	Air Quality System
AZ	Arizona
BCs	Boundary Conditions
CAMx	Comprehensive Air quality Model with extensions
CASNET	Clean Air Status and Trends Network
CB6r5	Carbon Bond version 6, Revision 5
CEMS	Continuous Emissions Monitoring System
CMAQ	Community Multiscale Air Quality Model
CONUS	CONtinental US
CRC	Coordinating Research Council
EBI	Euler Backward Iterative solver
EIs	Emission Inventories
EPA	Environmental Protection Agency
FNMOC	Fleet Numerical Meteorology and Oceanography Center
GAM	Generalized Additive Model
GEOS-Chem	Goddard Earth Observing System Chemical global model
GFAS	Global Fire Assimilation System
GIS	Geographic Information System
GOES	Geostationary Operational Environmental Satellite
HPMS	Highway Performance Monitoring System
HTTP	Hyper Text Transfer Protocol
ICs	Initial Conditions
IMPROVE	Interagency Monitoring of Protected Visual Environments
km	kilometer
MB	Mean Bias
MERRA	Modern-Era Retrospective analysis for Research and Applications
MLR	Multiple Linear Regression
MODIS	MODerate resolution Imaging SpectroRadiometer
MP	Modeling Platform
MPE	Model Performance Evaluation
NASA	National Aeronautics and Space Administration
NAA	Non Attainment Area
NAAQS	National Ambient Air Quality Standard
NAM	North American Model
NCAR	National Center for Atmospheric Research
netCDF	network Common Data Format
NLCD	National Land Cover Database
NMB	Normalized mean bias
NME	Normalized mean error (unsigned, or gross)
NOAA	National Oceanic and Atmospheric Administration
NOx	Nitrogen oxides
NPP	National Polar-orbiting Partnership

NTAD	National Transportation Atlas Database
OC	Organic Carbon
OMI	Ozone Monitoring Instrument
OMPS	Ozone Mapping and Profiler Suite
PBL	Planetary Boundary Layer
PGM	Photochemical Grid Model
PM	Particulate Matter
$PM_{2.5}$	Particulate Matter less than 2.5 microns
ppb	parts per billion
POC	Primary Organic Carbon
PPM	Piecewise Parabolic Method
RRTMG	Rapid Radiative Transfer Model for Global Applications
s	second
SIP	State Implementation Plan
SOA	Secondary Organic Aerosol
SOAP	Secondary Organic Aerosol thermodynamic Partitioning
SOAP3	Secondary Organic Aerosol thermodynamic Partitioning version 3
µg	microgram
US	United States
VIIRS	Visible Infrared Imaging Radiometer Suite
VOC	Volatile organic compounds
WRF	Weather Research and Forecasting model
YSU	Yonsei University

EXECUTIVE SUMMARY

The Coordinating Research Council (CRC) funded Ramboll to conduct Project A-137 to develop a novel methodology for utilizing satellite data to calibrate fine-grid (1 km) air quality simulations and estimate the source contribution of on-road vehicle emissions to fine particulate matter ($PM_{2.5}$) ground-level concentrations near highways and transportation corridors.

The Tropospheric Emissions: Monitoring of Pollution (TEMPO) surface $PM_{2.5}$ product is a promising new source of satellite data that can be used to estimate such $PM_{2.5}$ contributions from on-road vehicles. But as of this writing (August 2025), only one month of preliminary TEMPO surface $PM_{2.5}$ product has been released, and timing of future releases is uncertain. As a potential alternative to TEMPO, we investigated Aerosol Optical Depth (AOD) column data from Geostationary Operational Environmental Satellites (GOES) and Visible Infrared Imaging Radiometer Suite (VIIRS), but both have limitations (primarily low data completeness and interference from clouds and reflective surfaces) that prevent their use in this study.

Di et al. (2019) employed an ensemble-based model to estimate date-specific $PM_{2.5}$ concentrations across the contiguous United States at high spatial resolution. The main data sources include Moderate Resolution Imaging Spectroradiometer (MODIS) AOD satellite data, Ozone Monitoring Instrument (OMI) satellite NO_2 columns, total and speciated $PM_{2.5}$ surface measurements, Community Multiscale Air Quality (CMAQ) model concentrations, and Modern-Era Retrospective analysis for Research and Applications, Version 2 (MERRA2) modeled total and speciated $PM_{2.5}$ concentrations. The model predicts daily $PM_{2.5}$ concentrations at a resolution of 1 km x 1 km grid cells.

The most recent available data from this "$PM_{2.5}$ data product" is for calendar year 2016, which matches an available modeling year from EPA with 12 km grid resolution. We therefore developed a new modeling platform based on EPA's 2016 platform with spatially refined on-road mobile emissions for specific metropolitan areas to evaluate against the $PM_{2.5}$ data product.

We developed three Comprehensive Air Quality Model with Extensions (CAMx) 1 km domains that contain the urban areas of Phoenix, Dallas-Fort Worth and Baltimore-Washington. We selected these cities because they all have major highways and transportation corridors. Our $PM_{2.5}$ model performance evaluation compared our Base Case 1 km CAMx simulations, EPA's 12 km model results, and the $PM_{2.5}$ data product against available 24-hour $PM_{2.5}$ observations within each of the 3 urban areas. In all 3 domains, we found that our Base Case 1 km CAMx simulations increased $PM_{2.5}$ concentrations relative to the EPA 12 km simulations. For Phoenix, this increase was beneficial, as the EPA 12 km simulation underestimated $PM_{2.5}$ concentrations. However, the EPA 12 km simulations for Dallas-Fort Worth and Baltimore-Washington overestimated $PM_{2.5}$, so our Base Case 1 km CAMx simulations exacerbated these positive biases. For all 3 urban areas, the $PM_{2.5}$ data product showed excellent agreement with observations, meeting the Goal criteria (Emery et al., 2017) for bias and error in each area.

Our analysis of CAMx 1 km on-road vehicle pollution contributions to annual $PM_{2.5}$ showed hotspots that corresponded to transportation networks, but the pollution increases were inconsistent and patchy rather than extending continuously along entire roadways. These contributions were somewhat small (less than 2 $\mu g\ m^{-3}$) compared to the annual total $PM_{2.5}$ concentrations (8-20 $\mu g\ m^{-3}$ in urban locations near roadways). The spatial comparison of annual total $PM_{2.5}$ between CAMx and the $PM_{2.5}$ data product was somewhat poor. The CAMx $PM_{2.5}$ concentrations tended to be higher overall, and hotspots generally did not match up well between the two products. Neither of the two total $PM_{2.5}$ sets

of maps showed much roadway network signal, other than in West Phoenix, where other emission sectors are contributing.

Due to poor agreement between the CAMx simulation and the $PM_{2.5}$ data product, we were not able to gain useful information about emissions from Multiple Linear Regression (MLR) models developed for the three cities. The limitations of the modeling (12 km resolution for meteorology and most emission sectors, simple spatial interpolation technique applied to on-road and railway emissions, etc.) in this study likely play some role in the poor agreement between the CAMx results and the $PM_{2.5}$ data product.

While the $PM_{2.5}$ data product showed excellent agreement with $PM_{2.5}$ concentrations at monitor locations, we lack a methodology to evaluate the $PM_{2.5}$ data product away from monitor locations. Additionally, the data product is itself a model result (i.e. data fusion) rather than a direct observation. Nonetheless, MLR models could be deployed when a TEMPO other suitable $PM_{2.5}$ satellite product is made available.

We recommend the following for future work:

- Develop and evaluate a new CAMx modeling platform that uses high resolution meteorological simulations over one or more urban areas and "bottom-up" emissions processing at high resolution for on-road mobile and other sectors
- Develop new MLR models that evaluate $PM_{2.5}$ emissions from the new high-resolution CAMx simulations using TEMPO or another suitable satellite-based $PM_{2.5}$ product as they become available

1.0 INTRODUCTION

Emission inventories (EIs) and computer models are used to manage complex air quality issues such as $PM_{2.5}$ and ozone. The models provide a connection between ambient concentrations, which can be measured, and emission inventories, which are managed by regulations. However, traditional ambient concentration measurements at surface monitoring sites provide limited data coverage that poorly constrains uncertainties in the models and the EIs. Pollution mapping by aircraft and/or satellites can provide much more data that can then be used to improve the EIs and/or models.

The recently launched National Aeronautics and Space Administration (NASA) TEMPO satellite (discussed below) provides US-wide, hourly (during daylight and cloud-free periods), kilometer-scale data for $PM_{2.5}$ and ozone precursors (NO_2 and formaldehyde). Data for NO_2 and formaldehyde (HCHO) are available now but TEMPO $PM_{2.5}$ data are only available for August 2023 and have coarser spatial resolution than the TEMPO ozone precursor data, as described in more detail below. Ramboll looked for other satellite measurements of $PM_{2.5}$ over the US but found that the available data are too limited to meet the objectives of this study. Therefore, in consultation with CRC, we used a data fusion product from Di et al. (2019) that combines satellite data with other data to provide 1 km gridded, daily, US-wide surface $PM_{2.5}$ concentration estimates (Figure 1-1). Using these data allows us to develop and test methods that can be applied later to TEMPO or another suitable satellite-based $PM_{2.5}$ data product.

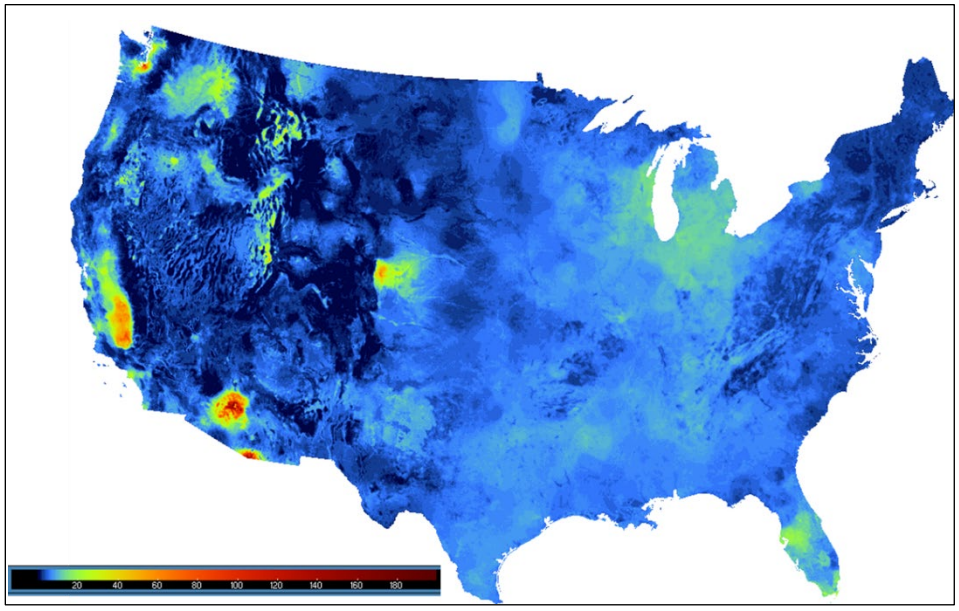

Figure 1-1. Example 1 km gridded surface $PM_{2.5}$ concentration ($\mu g/m^3$) for January 1, 2016, from Di et al., 2019.

1.1 Purpose

The CRC funded Ramboll to conduct Project A-137 to develop a novel methodology for utilizing satellite data to calibrate fine-grid (1 km) air quality simulations and estimate the source contribution of on-road vehicle emissions to $PM_{2.5}$ ground-level concentrations near highways and transportation corridors.

1.2 Background

1.2.1 TEMPO $PM_{2.5}$ Product

In December 2024, NASA Langley Atmospheric Science Data Center (ASDC) released TEMPO Version 03 (V03) Provisional NO_2 and HCHO satellite column measurements on a near real-time basis. As of this writing (August 2025), only one month (August 2023) of preliminary TEMPO surface $PM_{2.5}$ product has been released, and timing of future releases is uncertain. The TEMPO surface $PM_{2.5}$ product has coarser spatial resolution (8.0 km x 4.75 km) than both the TEMPO NO_2 and HCHO products (2.0 km x 4.75 km). This spatial resolution is too coarse to resolve features like highways and transportation corridors which are the focus of this study. Also, the methodology in calculating surface $PM_{2.5}$ concentrations from column measurements introduces additional assumptions that increase uncertainty and require validation.

1.2.2 Other Satellite $PM_{2.5}$ Products

As a potential alternative to TEMPO, we investigated AOD column data from Geostationary Operational Environmental Satellites (GOES) with 2.0 km x 2.0 km spatial resolution and 5-minute temporal resolution during daylight hours. We found low data completeness (<20%) due to clouds, highly reflective surfaces (desert landscapes, solar farms, roadways, etc.) and other factors. Fu et al. (2023) also found low data completeness (<15%) across North America.

Polar-orbiting satellite instruments such as Moderate Resolution Imaging Spectroradiometer (MODIS) and Visible Infrared Imaging Radiometer Suite (VIIRS) measure AOD at high spatial resolution (1 km x 1 km or finer) but can only make measurements once per day over a given location, typically in mid-morning or early afternoon. Similar to GOES, AOD measurements from these polar orbiter instruments are obscured by clouds and other factors. Thus, we cannot find a pure satellite $PM_{2.5}$ or AOD data product to use for this study.

1.2.3 Hybrid 1 km $PM_{2.5}$ data product

Di et al. (2019) employed an ensemble-based model to estimate date-specific $PM_{2.5}$ concentrations across the contiguous United States with high spatial resolution. Their model integrates three distinct machine learning techniques: neural network, random forest, and gradient boosting, leveraging a variety of predictor variables. Predictions from each of the machine learning techniques were obtained and integrated using a geographically weighted generalized additive model (GAM) as an ensemble model to create a combined $PM_{2.5}$ estimation. The main data sources include MODIS AOD (Aerosol Optical Depth) satellite data, OMI satellite NO_2 columns, total and speciated $PM_{2.5}$ surface measurements, Community Multiscale Air Quality (CMAQ) model concentrations, and Modern-Era Retrospective analysis for Research and Applications, Version 2 (MERRA2) modeled total and speciated $PM_{2.5}$ concentrations. In addition, terrain elevation data, road density, and land-use variables from the National Land Cover Database (NLCD) are considered. Meteorological variables such as air temperature, accumulated total precipitation, planetary boundary layer height, cloud area fractions, precipitable water, pressure, specific humidity, visibility, wind speed, and albedo are also incorporated into the model. The model predicts daily $PM_{2.5}$ concentrations at a resolution of 1 km x 1 km grid cells.

The ensemble model was validated using a 10-fold cross-validation method, which involved dividing the data into ten subsets. For each iteration, the model was trained on nine subsets and tested on the remaining subset to ensure comprehensive validation across different data points. This approach yielded a cross-validated R^2 of 0.86 for daily $PM_{2.5}$ predictions and 0.89 for annual estimates, indicating good model performance. The predictions were also evaluated against $PM_{2.5}$ monitoring data to ensure robustness. The $PM_{2.5}$ monitoring data used for validation were obtained from various sources, including the Air Quality System (AQS) operated by the Environmental Protection Agency

(EPA), The Interagency Monitoring of Protected Visual Environments (IMPROVE), Clean Air Status and Trends Network (CASTNET), and other regional or local datasets. These data encompassed measurements from 2,156 monitoring sites, providing 24-hour averaged $PM_{2.5}$ concentrations across diverse regions and timeframes. To enhance the model's accuracy and leverage spatial autocorrelation, spatially lagged monitored $PM_{2.5}$ values were incorporated as predictor variables. These lagged values consisted of weighted averages from nearby monitoring sites, with weights inversely proportional to distance and the distance squared.

For this study, we used version 1.10 of these 1 km gridded daily $PM_{2.5}$ concentrations, which we refer to hereafter as the "$PM_{2.5}$ data product". In this version, the completeness of daily $PM_{2.5}$ predictions was improved by using linear interpolation to address and fill in missing values. For instances where small spatial gaps of missing data occurred (i.e., under 100 grid cells with missing data), inverse distance weighting interpolation was applied to populate these gaps. For other instances of missing daily $PM_{2.5}$ data, values were interpolated from the nearest days with existing data.

The most recent available data from this product is for calendar year 2016, which matches an available CMAQ/CAMx modeling year from EPA with 12 km grid resolution. We therefore developed a new modeling platform based on EPA's 2016 platform with spatially refined on-road mobile emissions for specific metropolitan areas to evaluate against the hybrid satellite $PM_{2.5}$ product.

1.2.4 CAMx Modeling Platform

We selected the EPA 2016v3 modeling platform (MP; Eyth et al., 2023) for calendar year 2016 because it is a mature and well-tested database with 12 km grid resolution over the continental US (CONUS), and it matches the most recent year available (also 2016) of the Di et al. $PM_{2.5}$ data product. We chose CAMx because its meteorological interface processor – WRFCAMx – provides the capability of interpolating EPA's Weather Research and Forecast model (WRF) meteorological inputs from 12 km to 1 km resolution for the focus areas of this study. We interpolated and spatially subset EPA's gridded emissions from 12 km to 1 km. Simple interpolation of emissions from highways and transportation corridors using would not be unsuitable for project objectives and so we used more advanced interpolation methods, as described below.

2.0 DEVELOPMENT OF HIGH-RESOLUTION CAMX MODELING PLATFORM

This chapter discusses the procedures for developing a photochemical grid model (PGM) database for evaluation of model performance and comparison to the 2016 EPA modeling platform and $PM_{2.5}$ data product.

2.1 Horizontal Modeling Domains

We developed three CAMx 1 km domains that contain the urban areas of Phoenix (Figure 2-1), Dallas-Fort Worth (Figure 2-2) and Baltimore-Washington (Figure 2-3). We selected these cities because they all have major highways and transportation corridors. Additionally, we avoided cities with complex terrain where 12 km meteorology from the EPA 2016v3 12 km modeling platform (MP) would be inadequate to resolve source-receptor relationships.

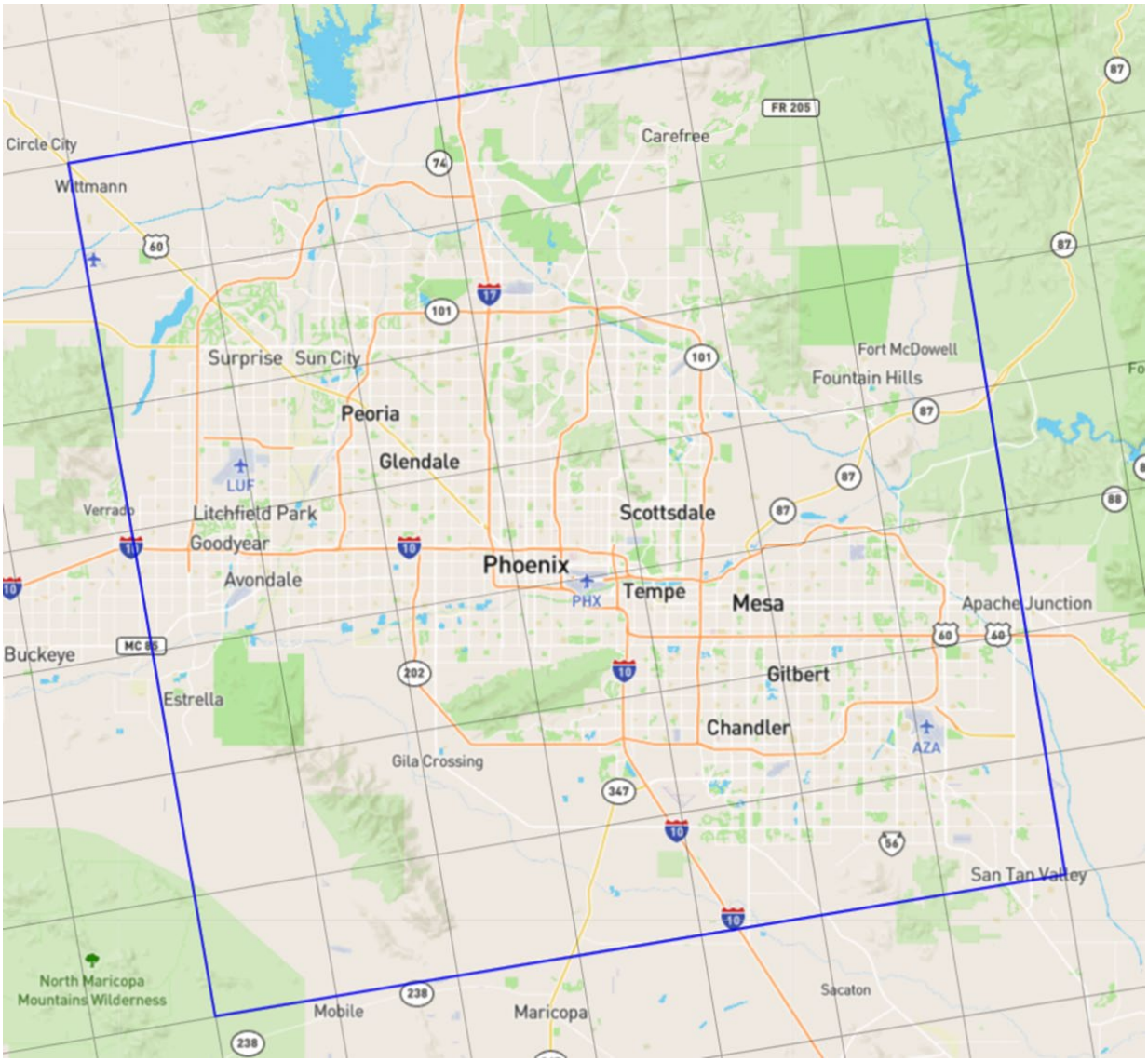

Figure 2-1. Phoenix 1 km CAMx domain (blue) with EPA 12 km grid cells overlaid for reference.

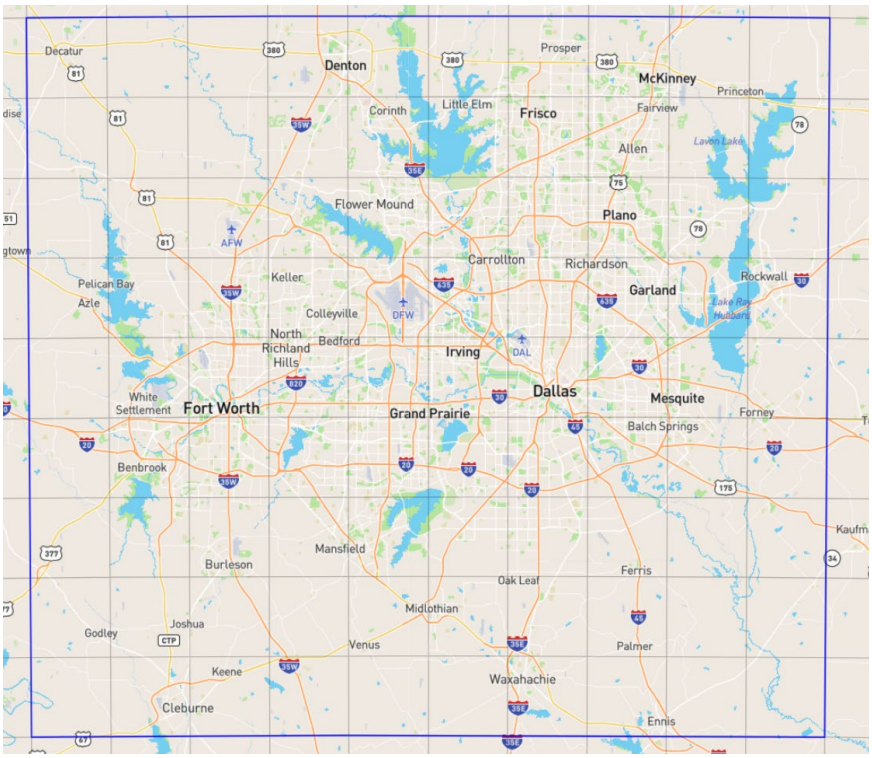

Figure 2-2. Dallas-Fort Worth 1 km CAMx domain (blue) with EPA 12 km grid cells overlaid for reference.

Figure 2-3. Baltimore-Washington 1 km CAMx domain (blue) with EPA 12 km grid cells overlaid for reference.

2.2 Vertical Layer Structure

The CAMx vertical layer structure is defined by the vertical levels used in EPA's 2016v3 MP. EPA runs WRF with 35 vertical levels from the surface to 50 mb height as shown in Table 2-1. CAMx has the same vertical structure as WRF and uses 34 vertical layers with the lowest layer 1 being 19 m thick.

Table 2-1. 34 layer vertical structure used in EPA's WRF modeling that was also used for CAMx in this study.

WRF Layer	Height (m)	Pressure (mb)	Sigma
35	17,556	5000	0.000
34	14,780	9750	0.050
33	12,822	14500	0.100
32	11,282	19250	0.150
31	10,002	24000	0.200
30	8,901	28750	0.250
29	7,932	33500	0.300
28	7,064	38250	0.350
27	6,275	43000	0.400
26	5,553	47750	0.450
25	4,885	52500	0.500
24	4,264	57250	0.550
23	3,683	62000	0.600
22	3,136	66750	0.650
21	2,619	71500	0.700
20	2,226	75300	0.740
19	1,941	78150	0.770
18	1,665	81000	0.800
17	1,485	82900	0.820
16	1,308	84800	0.840
15	1,134	86700	0.860
14	964	88600	0.880
13	797	90500	0.900
12	714	91450	0.910
11	632	92400	0.920
10	551	93350	0.930
9	470	94300	0.940
8	390	95250	0.950
7	311	96200	0.960
6	232	97150	0.970
5	154	98100	0.980
4	115	98575	0.985
3	77	99050	0.990
2	38	99525	0.995
1	19	99763	0.9975
Surface	0	100000	1.000

2.3 Meteorological Inputs

We obtained EPA's WRF outputs for the CONUS 12 km domain from their 2016v3 modeling platform. We then used the WRFCAMx interface processor to generate CAMx meteorological inputs by subsetting and interpolating the WRF outputs to the CAMx 1 km domains shown in Section 2.1.

2.3.1 EPA WRF 2016 12 km Domain Simulation

Table 2-2 summarizes the EPA 12 km WRF configuration used in this study. We lacked resources to conduct a model performance evaluation specific to each of the three cities. EPA provides more detailed information about the WRF configuration as well as a summary of WRF performance in EPA (2019).

Table 2-2. EPA 2016 12 km WRF configuration used in the CRC A-137 study.

WRF Option	EPA
Domains run	Continental US 12 km
Vertical Coordinate	Hybrid
Microphysics	Morrison 2
Longwave Radiation	Rapid Radiative Transfer Model for Global Applications (RRTMG)
Shortwave Radiation	RRTMG
Surface Layer Physics	Pleim-Xiu
Land Surface Model	Pleim-Xiu
Planetary Boundary Layer scheme	Asymmetric Convective Model version 2 (ACM2)
Cumulus	Kain-Fritsch
Boundary and Initial Conditions and Analysis Nudging Source	12 km North American Model (NAM)
Analysis Nudging	On
Observation Nudging	None
Sea Surface Temperature	Fleet Numerical Meteorology and Oceanography Center (FNMOC)

2.4 Initial Concentration and Boundary Condition Inputs

We extracted initial and boundary concentrations (ICs and BCs) from a 3-D CAMx run over EPA's 12US2 (CONUS) domain that used EPA's 2016 modeling platform. EPA's modeling platform used GEOS-Chem for its boundary and initial condition dataset. We initialized CAMx 10 days prior to January 1, 2016 to wash out the influence of the initial concentrations.

2.5 Emission Inputs

We disaggregated 12 km CAMx model-ready on-road and rail emissions to 1 km resolution using shapefiles. For on-road emissions, we used Annual Average Daily Traffic (AADT) from 2017 Highway Performance Monitoring System (HPMS) shapefiles. For rail emissions, we used raster density surface of railroads (DENS) from 2014 National Transportation Atlas Database (NTAD) shapefiles. This approach is efficient and preserves the temporal allocation and chemical speciation present in the 2016v3 while enhancing spatial resolution. Point sources require no spatial refinement because they already have point locations.

Remaining emission categories, e.g., area sources and biogenic emissions, would derive less benefit from spatial refinement because they are spatially dispersed with distributions that are poorly characterized. However, we did refine their spatial allocations to avoid placing land-based emissions (e.g., biogenic emissions) in over-water 1 km grid cells. As an example, we provide the land fraction map for the Baltimore-Washington CAMx 1 km domain used to reallocated land-based emissions.

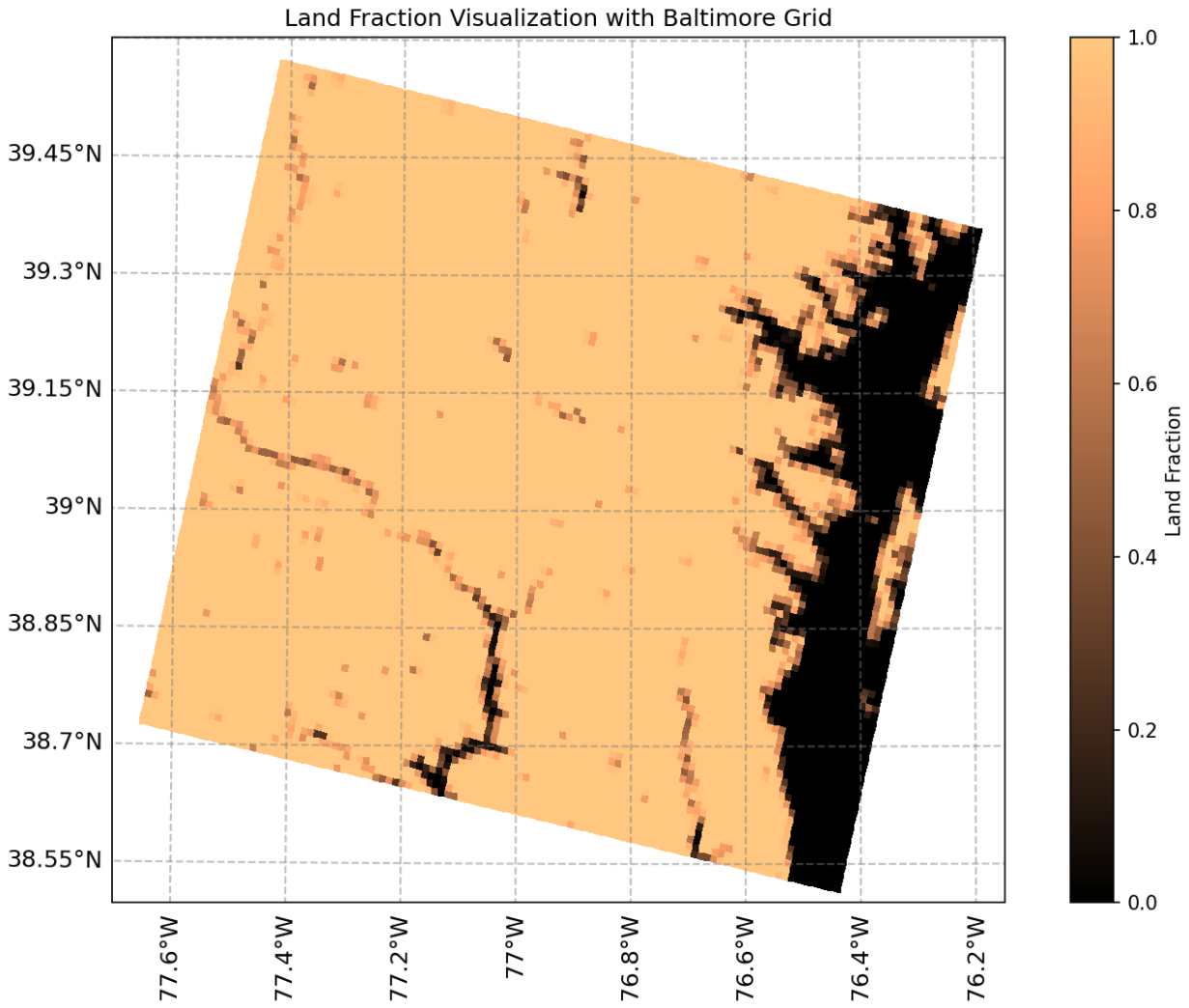

Figure 2-4. Land fraction map for CAMx 1 km Baltimore-Washington domain.

2.6 CAMx Ancillary Inputs

Total atmospheric ozone column data are needed to derive clear-sky photolysis rate inputs for CAMx. These data are available every 24 hours from the Ozone Mapping and Profiler Suite (OMPS) aboard the joint NASA/NOAA Suomi National Polar-orbiting Partnership (Suomi NPP) satellite and are distributed on an HTTP site supported by the National Aeronautics and Space Administration (NASA; 2023). This ozone data is processed for the CAMx parent domain by the O3MAP processor. The O3MAP outputs are then used by the TUV[1] radiative transfer and photolysis model, developed and distributed by the National Center of Atmospheric Research (NCAR; 2011), to provide the air quality model with a multi-dimensional lookup table of clear-sky photolysis rates. CAMx internally adjusts clear-sky rates for the presence of clouds and aerosols using a fast in-line version of TUV.

Rather than relying on landuse files developed from EPA's WRF outputs (12 km resolution), we instead developed new 1 km fractional landuse files for each of the three CAMx domains. We configured WRF's geogrid processor to use the 2011 National Land Cover Dataset (NLCD[2]) that EPA used in their 2016

[1] https://www2.acom.ucar.edu/modeling/tropospheric-ultraviolet-and-visible-tuv-radiation-model
[2] https://www.mrlc.gov/data/nlcd-2011-land-cover-conus

WRF simulation. The Multi-Resolution Land Characteristics Consortium developed the NLCD dataset and is based on observations from the Landsat Thematic Mapper (Homer et al., 2015). NLCD contains 20 landuse categories specific to the Continental U.S. and MODIS landuse categories elsewhere (Ran et al., 2015).

2.7 Summary of CAMx Options

Table 2-3 displays a summary of the options used in the CAMx 2016 1 km simulations. The latest publicly available version of CAMx (v7.31; released in August 2024) was used with the SOAP3 secondary organic aerosol (SOA) module to isolate the effects of treating the semi-volatility of primary emitted carbon (POC) from fires. The CB6r5 gas-phase chemistry, coarse/fine aerosol treatment, Zhang dry deposition scheme and PPM advection solver were used.

Table 2-3. CAMx model configuration used in CRC Project A-137 modeling of 2016.

Science Options	CAMx	Comment
Model Code	CAMx v7.31	With SOAP3, August 2024
Horizontal Grid Mesh	1 km	
Phoenix	84 x 84 cells	
Dallas-Fort Worth	120 x 88 cells	
Baltimore-Washington	108 x 96 cells	
Vertical Grid Mesh	34 vertical layers	Layer 1 = 19 m. Model top 50 mb.
Initial Conditions	10-day spin-up end of Dec 2015	
Boundary Conditions	CAMx run using 2016 EPA Modeling Platform; Boundary conditions outside US from GEOS-Chem	
Emissions		
Baseline Emissions	EPA 2016v3 Emissions Modeling Platform (EMP)	Original point source emissions unaltered; Gridded emissions at 12 km resolution for all sectors besides on-road mobile and railway
On-road Mobile Emissions	Regridded to 1 km domains	Used Annual Average Daily Traffic (AADT) from 2017 Highway Performance Monitoring System (HPMS) shapefiles
Railway Emissions	Regridded to 1 km domains	Used raster density surface of railroads (DENS) from 2014 National Transportation Atlas Database (NTAD) shapefiles
Chemistry		
Gas Phase Chemistry	CB6r5	Updated CB6 chemistry revision 5
Aerosol Scheme	Coarse/Fine	
Secondary Organic Aerosol	SOAP3	SOAP3 updated semi-volatile treatment of POC
Meteorology		
Source of WRF	EPA WRF CONUS 12 km	
Meteorological Processor	WRFCAMx	Use YSU vertical diffusion coefficient
Horizontal Diffusion	Spatially varying	K-theory with Kh grid size dependence
Vertical Diffusion	YSU Kv formulation	Minimum Kv 0.1 to 1.0 m^2/s
Diffusivity Lower Limit	Kv_min = 0.1 to 1.0 m^2/s	Depends on percent urban landuse
Deposition Schemes		
Dry Deposition	Zhang dry deposition scheme	(Zhang et al., 2001; 2003)
Wet Deposition	CAMx -specific formulation	rain/snow/graupel
Numerics		
Gas Phase Chemistry Solver	Euler Backward Iterative (EBI)	EBI fast and accurate solver
Vertical Advection Scheme	Implicit scheme	
Horizontal Advection Scheme	Piecewise Parabolic Method (PPM) scheme	Colella and Woodward (1984)
Integration Time Step	Wind speed dependent	1-5 min

3.0 $PM_{2.5}$ MODEL PERFORMANCE EVALUATION AND ANALYSIS

3.1 Testing Database

We configured the Atmospheric Model Evaluation Tool (AMET) to evaluate the Base Case CAMx runs, EPA's 2016 run and the $PM_{2.5}$ data product for the 2016 annual modeling period. AMET matches the model output at grid cells that collocate with observational sites for one or more monitoring networks. We used the same set of $PM_{2.5}$ monitoring data for each of the three products (Base Case 1 km CAMx, EPA 12 km and $PM_{2.5}$ 1 km data product) in each urban area. AMET also performs species mappings to match the modeled species to those from corresponding observations. These model and observation pairings are then used to analyze the model's performance using a variety of statistical and graphical techniques. Table 3-1summarizes key statistical measures that were used to quantify model performance. We focused the evaluation on total $PM_{2.5}$ concentrations.

Table 3-1. Model Performance Evaluation Metrics.

Metric	Definition
Mean observation value	The average observed concentration
Mean simulation value	The average simulated concentration
Normalized bias (NMB)	$\sum_{l=1}^{N}(S_l - O_l)/O_l \cdot 100\%$
Normalized error (NME)	$\sum_{l=1}^{N}\lvert S_l - O_l\rvert/O_l \cdot 100\%$
Where, N is the number of data pairs, and S_l and O_l are the simulated and observed values at site *l*, respectively, over a given time interval	

3.2 Model Performance Goals and Benchmarks

EPA first proposed the use of ozone model performance goals in their 1991 ozone modeling guidance (EPA, 1991) with goals for bias (≤± 15%) and error (≤ 35%). Since then, EPA has lessened the emphasis on the use of model performance goals as some users focused on achieving the model performance goals and not whether the model was correctly simulating atmospheric processes that led to the high ozone concentrations. However, model performance goals are still useful for interpreting model performance and putting the model performance into context. Boylan and Russell (2006) extended the performance goals to PM species and visibility. Simon et al. (2012) summarized the model performance statistics of 69 PGM applications from 2006 to 2012 and although they found significant variability, they were able to isolate model performance statistical levels for the best performing models.

Emery et al. (2017) built off the work of Simon et al. (2012) including additional PGM model applications and recommended a set of PGM model performance goals and criteria based on the variability of past model performance. "Goals" indicate statistical values that about a third of the top performing past PGM applications have met and should be viewed as the best a model can be expected to achieve. "Criteria" indicates statistics values that about two thirds of past PGM applications have met and should be viewed as what most models have achieved. In the following

section, we compare model performance statistics for normalized mean bias (NMB) and normalized mean error (NME) for each of the Base Case 1 km CAMx, EPA 12 km and $PM_{2.5}$ 1 km data product for the three urban areas against the model performance goals and criteria summarized by Emery et al. (2017) that are given in Table 3-2.

Table 3-2. Recommended benchmarks for photochemical model statistics for $PM_{2.5}$ (Source: Emery et al., 2017).

Species	NMB		NME		r	
	Goal	Criteria	Goal	Criteria	Goal	Criteria
24-hr $PM_{2.5}$	<±10%	<±30%	<35%	<50%	>0.70	>0.40

3.3 $PM_{2.5}$ Model Performance Evaluation Comparison

In Figure 3-1, we present scatter plots that show 24-hour $PM_{2.5}$ concentrations across the entire 2016 modeling period for the Phoenix Base Case (1 km; left panel), EPA 2016 MP (12 km; middle) and $PM_{2.5}$ data product (1 km; right). EPA's run shows a negative bias overall (MB: -2.4 μg m^{-3}), which is improved substantially in the Base Case 1 km run (MB: +0.7 μg m^{-3}). The Base Case run meets the Goal benchmark (<±10%) for NMB (+8.3%) and the Criteria benchmark (<50%) for NME (+42.3%). The $PM_{2.5}$ data product has 24-hour $PM_{2.5}$ concentrations from AQS monitoring sites as its primary input, so the very good agreement with observations (MB: -0.5 μg m^{-3}; NMB and NME within Goal benchmarks) is not surprising. Still, there are some outliers (both over and underestimates), which suggest the data product could have trouble with short-lived (windblown dust, e.g.) events.

Figure 3-2 shows a similar scatter plot, but for the Dallas-Fort Worth modeling domain. In this region, the EPA 12 km run shows good performance (MB: +0.6 μg m^{-3} and NMB/NME within Goal benchmarks) and the Base Case is slightly worse (MB: +1.7 μg m^{-3} and NMB/NME outside Goal but within Criteria benchmarks). We attribute this increased positive bias relative the EPA run to the 1 km resolution and refinement of on-road and rail emissions. As seen with the Phoenix results, the $PM_{2.5}$ data product shows excellent agreement with observations with minimal bias (MB: -0.2 μg m^{-3}) and NMB/NME both within the Goal benchmarks.

Figure 3-3 shows similar scatter plots for the Baltimore-Washington modeling domain. The EPA 12 km run shows the largest bias (+4.9 μg m^{-3}), and overall worst agreement (NMB: +60.3%; NME: 63.9%) with observations across the three cities. As with Phoenix and Dallas-Fort Worth, the Base Case 1 km run increases modeled $PM_{2.5}$ concentrations, so the large positive bias in the EPA 12 km run is made worse (MB: +7.7 μg m^{-3}). Again, the $PM_{2.5}$ data product shows excellent agreement with observations (MB: -0.3 μg m^{-3} and NMB/NME within Goal benchmark).

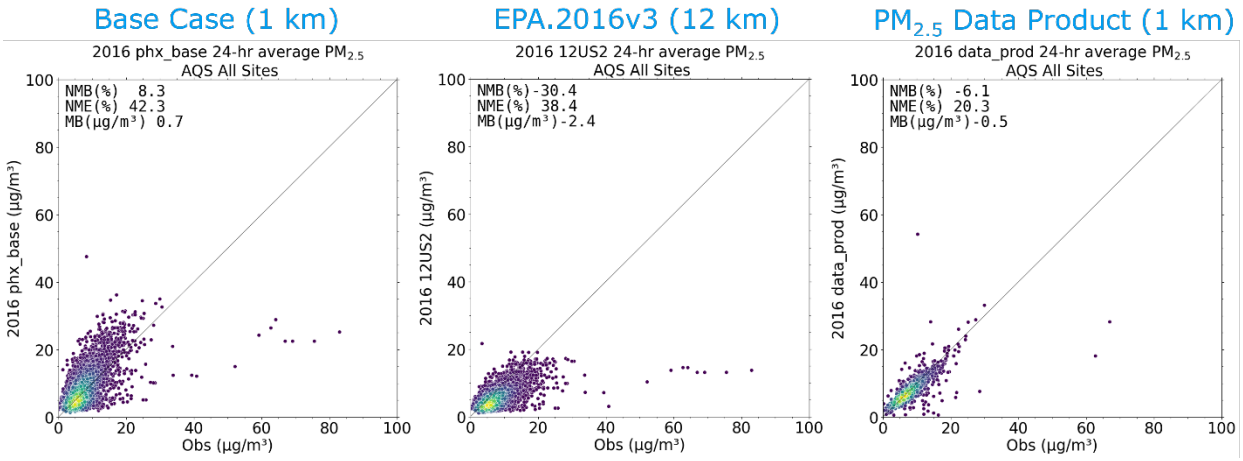

Figure 3-1. Scatter plots showing 24-hour $PM_{2.5}$ concentrations for Phoenix Base Case (left panel), EPA.2016v3 (middle panel) and $PM_{2.5}$ data product (right panel) against observations.

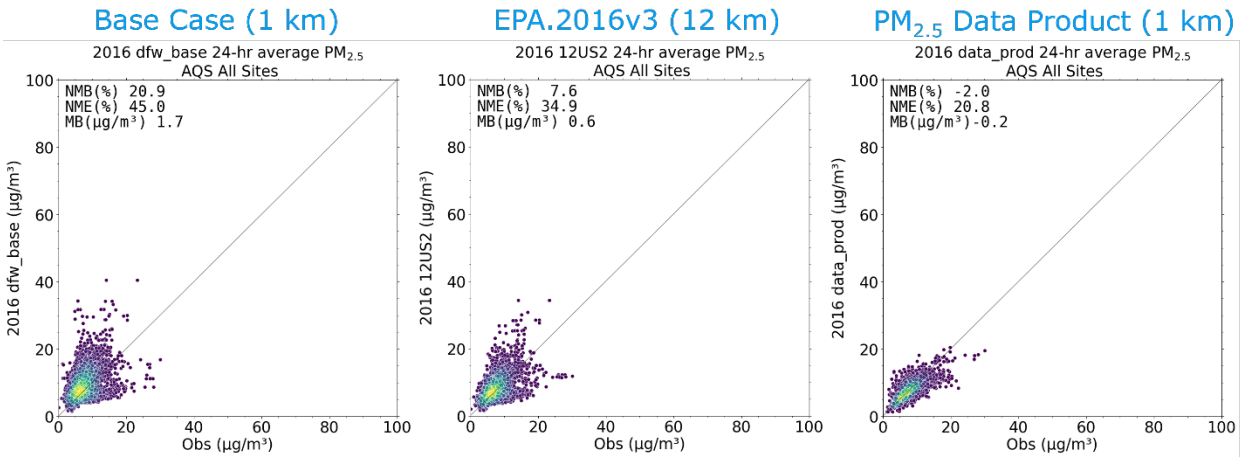

Figure 3-2. Scatter plots showing 24-hour $PM_{2.5}$ concentrations for Dallas-Fort Worth Base Case (left panel), EPA.2016v3 (middle panel) and $PM_{2.5}$ data product (right panel) against observations.

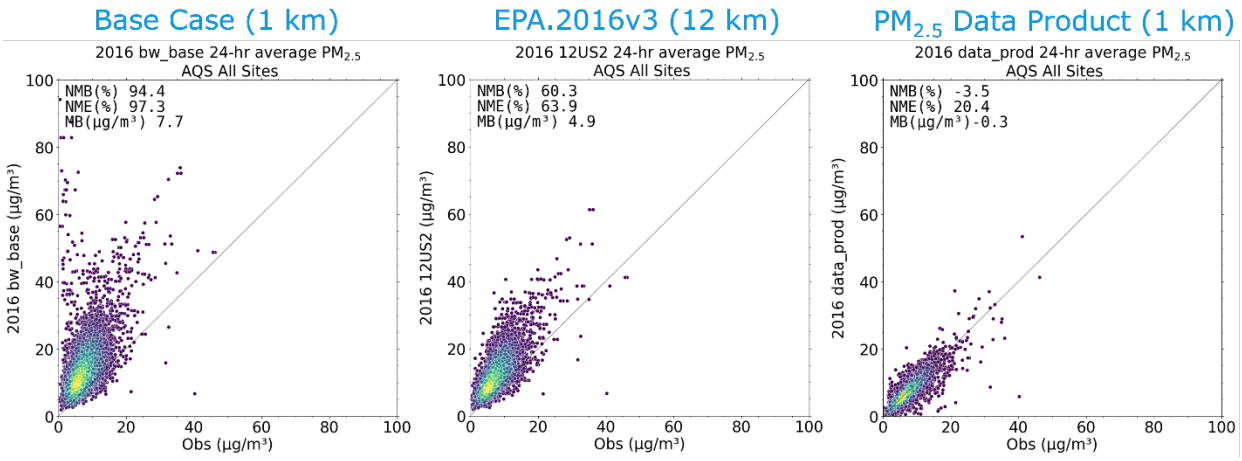

Figure 3-3. Scatter plots showing 24-hour $PM_{2.5}$ concentrations for Baltimore-Washington Base Case (left panel), EPA.2016v3 (middle panel) and $PM_{2.5}$ data product (right panel) against observations.

3.4 Comparison of Spatial Maps

We determined the contribution of on-road vehicles to annual $PM_{2.5}$ concentrations from the difference between the CAMx Base Case and On-road zero-out simulations. In this section, we show maps with this on-road contribution to annual $PM_{2.5}$ in each subdomain to reveal how well the 1 km grid resolution can resolve $PM_{2.5}$ near highways and transportation corridors. For comparison, we will also present similar maps of the total annual $PM_{2.5}$ for both the CAMx Base Case and the $PM_{2.5}$ data product.

3.4.1 Phoenix

Figure 3-4 shows the CAMx on-road mobile contribution to 2016 annual average $PM_{2.5}$ concentrations for the Phoenix 1 km CAMx domain. The spatial pattern shows $PM_{2.5}$ enhancements along roadways, but they appear as 1-cell "hotspots" rather than line segments of grid cells. Examining CAMx total $PM_{2.5}$ concentrations in Phoenix (see top panel of Figure 3-5), we find some hotspots along I-10 collocated with the roadway enhancements in the previous figure. Because the total $PM_{2.5}$ concentrations are much larger (10-12 µg m^{-3}) than the on-road mobile contribution (1-2 µg m^{-3}), we conclude that other emission sectors must also be contributing to $PM_{2.5}$ in this area. Comparing CAMx to the $PM_{2.5}$ data product (bottom panel of Figure 3-5), we find generally lower $PM_{2.5}$ in the data product (note maximum in color scale is also lower, to better identify roadway enhancements). However, the $PM_{2.5}$ concentrations in downtown Phoenix are similar (8-9 µg m^{-3}). The data product also reveals a more consistent pattern of higher $PM_{2.5}$ along the road networks, especially in areas outside of the city (AZ 202 Loop near Chandler).

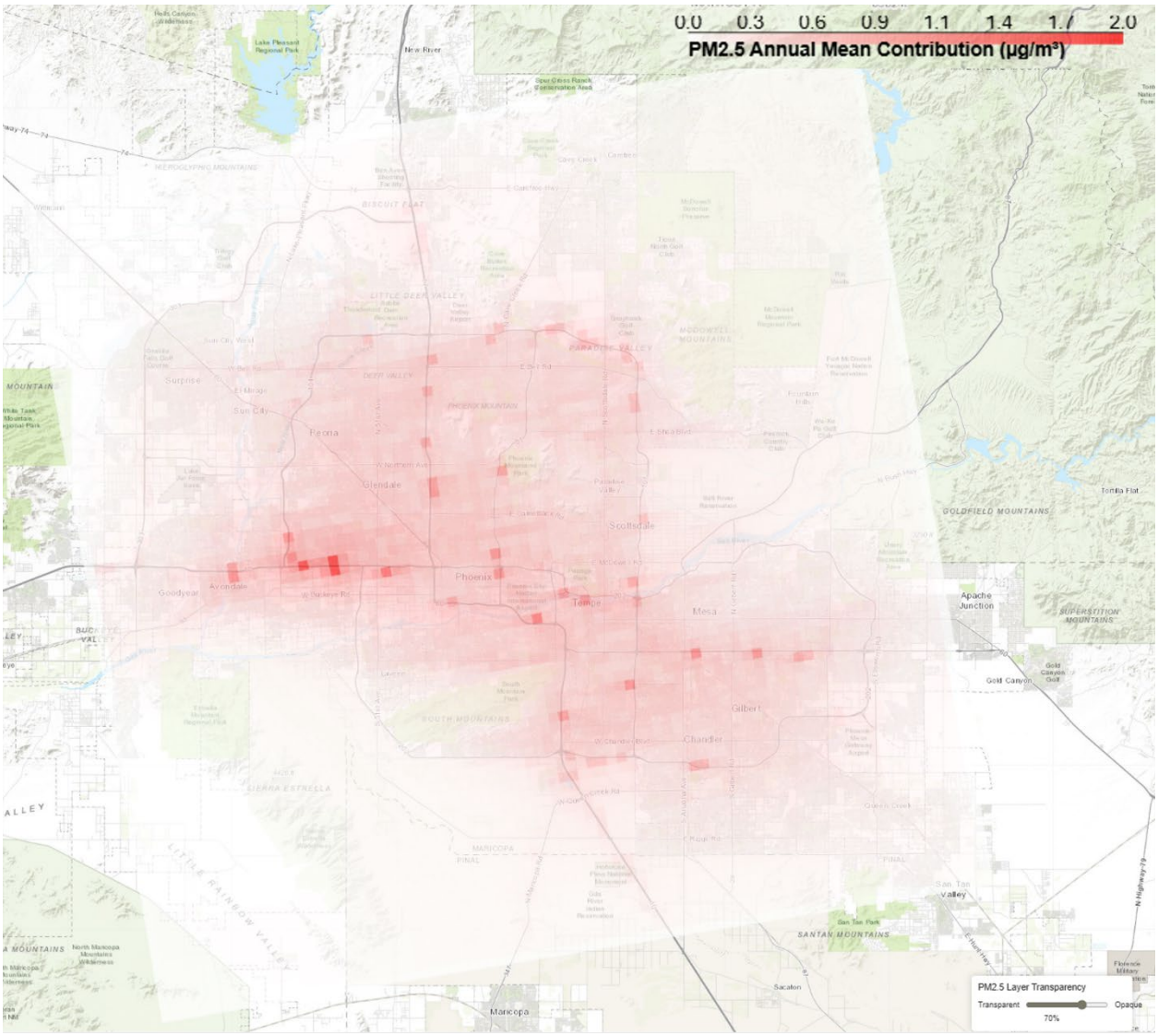

Figure 3-4. On-road mobile contribution to 2016 annual average total $PM_{2.5}$ concentrations for Phoenix 1 km CAMx domain.

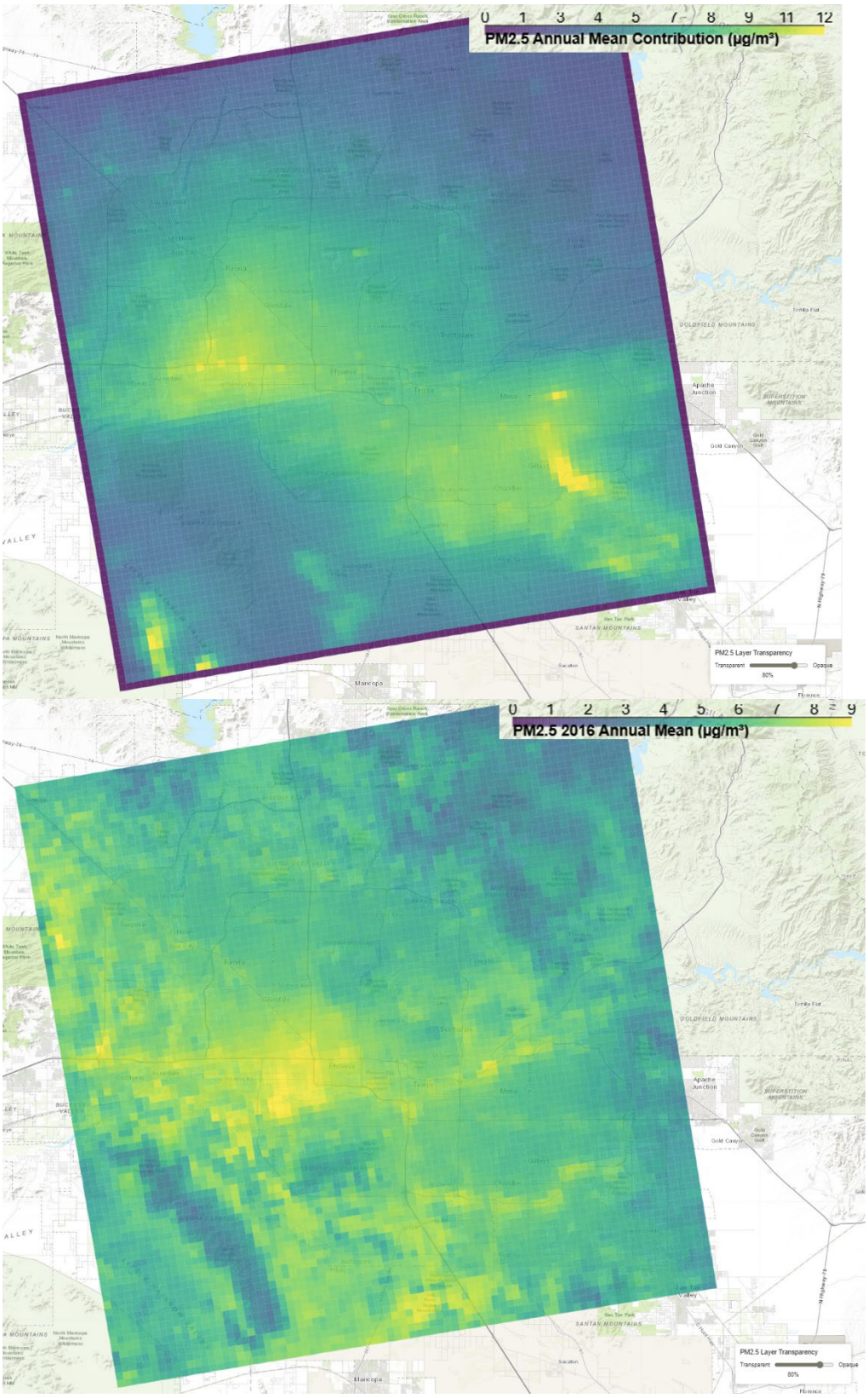

Figure 3-5. 2016 annual average total $PM_{2.5}$ concentrations for Base Case CAMx (top) and $PM_{2.5}$ data product (bottom) for Phoenix domain.

3.4.2 Dallas-Fort Worth

We present the same two figures as in the last section in Figure 3-6 and Figure 3-7, but for the Dallas-Fort Worth domain. Compared to Phoenix, Figure 3-6 shows more consistent alignment of $PM_{2.5}$ hotspots along the road networks, particularly around Dallas. However, similar to Phoenix, the on-road mobile contribution is small compared to the CAMx total $PM_{2.5}$ concentration map (top panel of Figure 3-7). We find no obvious enhancement along roadways for either CAMx total $PM_{2.5}$ or the $PM_{2.5}$ data product (bottom panel of Figure 3-7). Additionally, there is poor agreement between CAMx and the $PM_{2.5}$ data product. There is a substantial $PM_{2.5}$ hotspot (10-15 $\mu g\ m^{-3}$) in the southwest part of the domain (south of Fort Worth) that shows no such enhancement in the $PM_{2.5}$ data product.

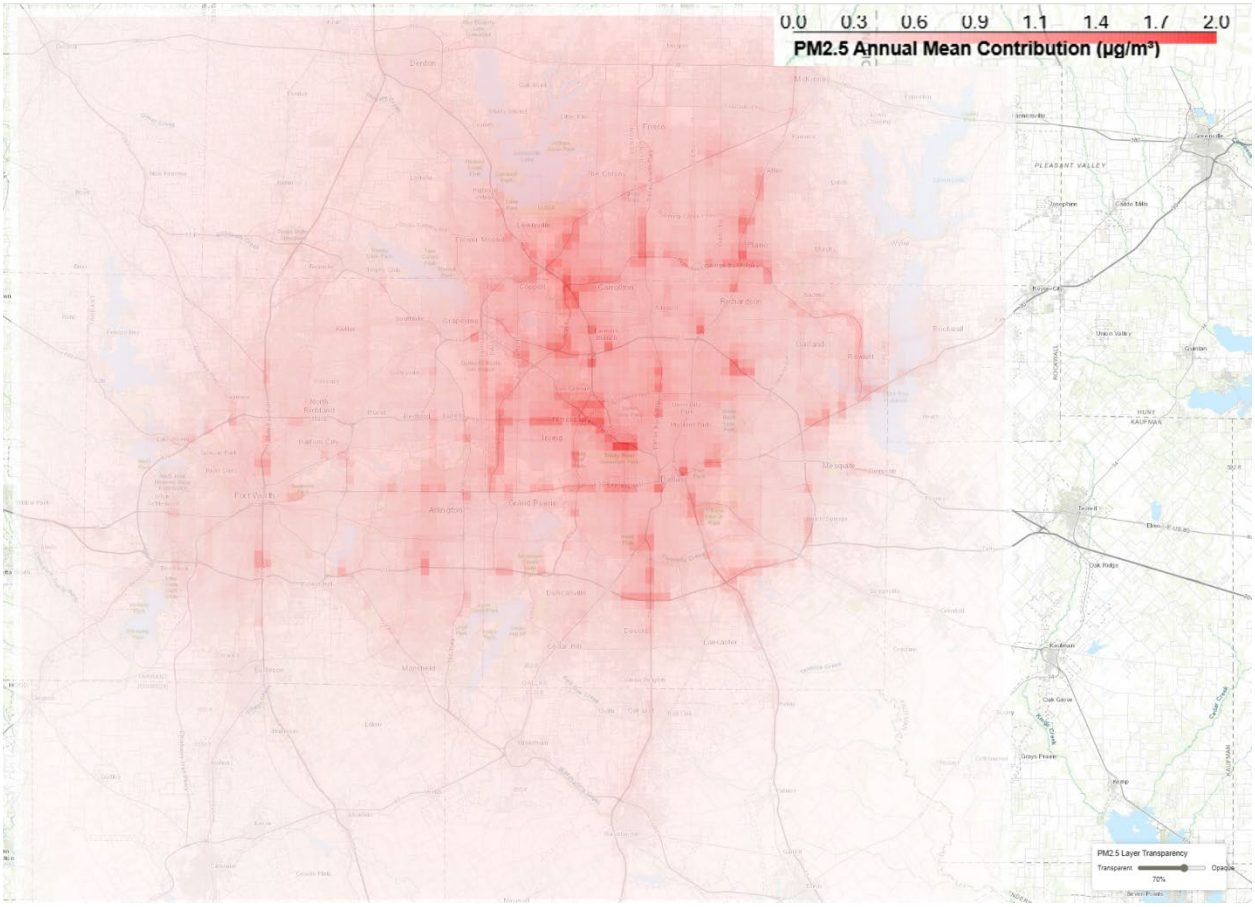

Figure 3-6. CAMx 1 km on-road mobile contribution to 2016 annual average total $PM_{2.5}$ concentrations for Dallas-Fort Worth domain.

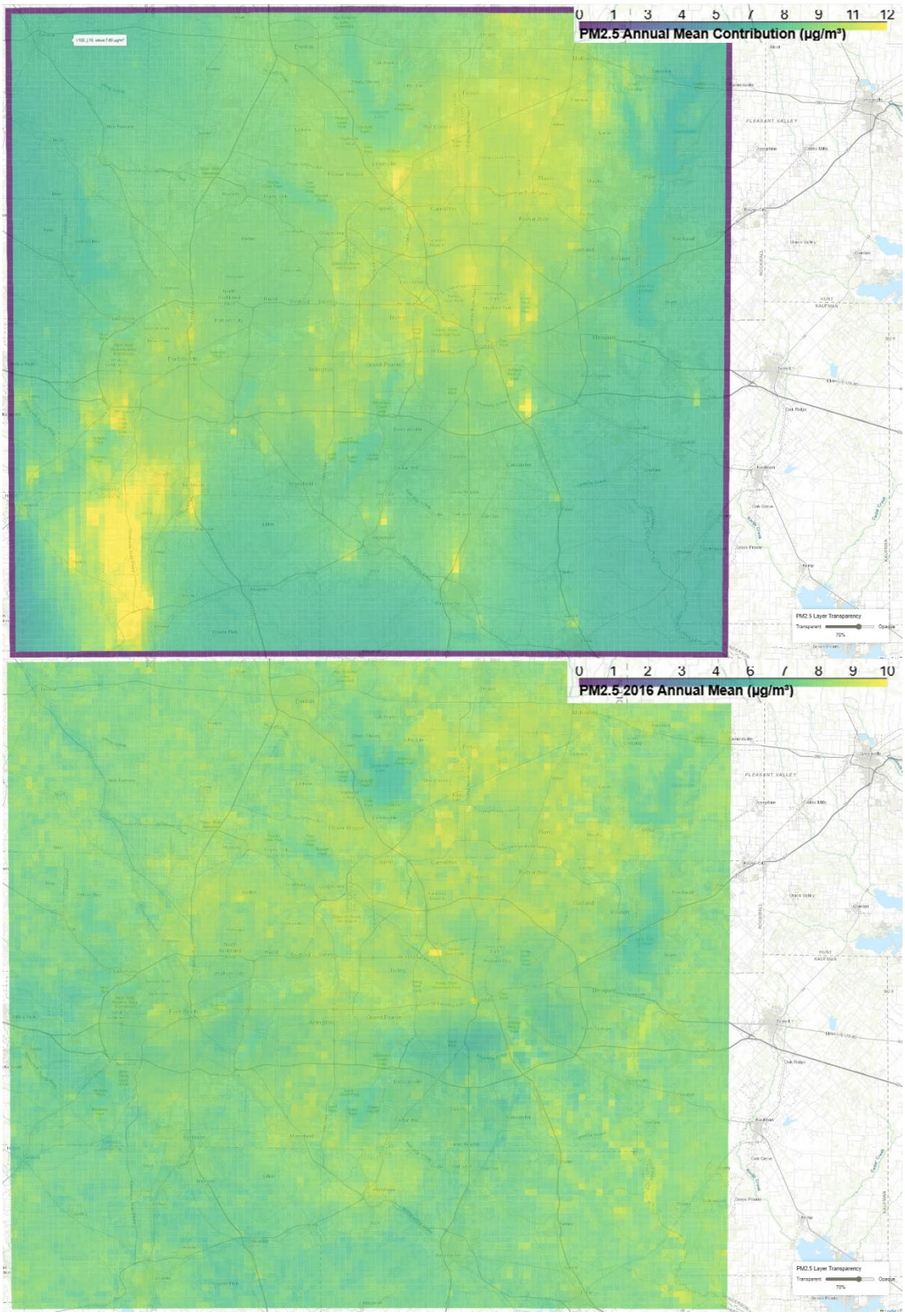

Figure 3-7. 2016 annual average total $PM_{2.5}$ concentrations for Base Case CAMx (top) and $PM_{2.5}$ data product (bottom) for Dallas-Fort Worth domain.

3.4.3 Baltimore-Washington

The Baltimore-Washington on-road mobile contribution to annual average $PM_{2.5}$ (Figure 3-8) shows higher $PM_{2.5}$ contributions (over 2.0 μg m^{-3}) than either Phoenix or Dallas-Fort Worth. However, because the CAMx total $PM_{2.5}$ concentrations (top panel of Figure 3-9) are even larger than in the other 2 cities, the on-road mobile contribution does not show up clearly. In this map, there are blocky outlines which indicate the importance of emission sectors that were not re-processed from 12 to 1 km (any sectors other than on-road mobile and rail emissions). While the CAMx results show general areas of $PM_{2.5}$ enhancement in and around Washington, D.C. and Baltimore, the $PM_{2.5}$ data product shows the highest $PM_{2.5}$ concentrations in between the 2 cities. This hotspot may be a signal of increased emissions along this traffic corridor, or it may reflect an artifact of the data fusion process used to create the $PM_{2.5}$ data product. Outside of this area, there appears to be slight enhancements along roadways, which are not found in the CAMx $PM_{2.5}$ map.

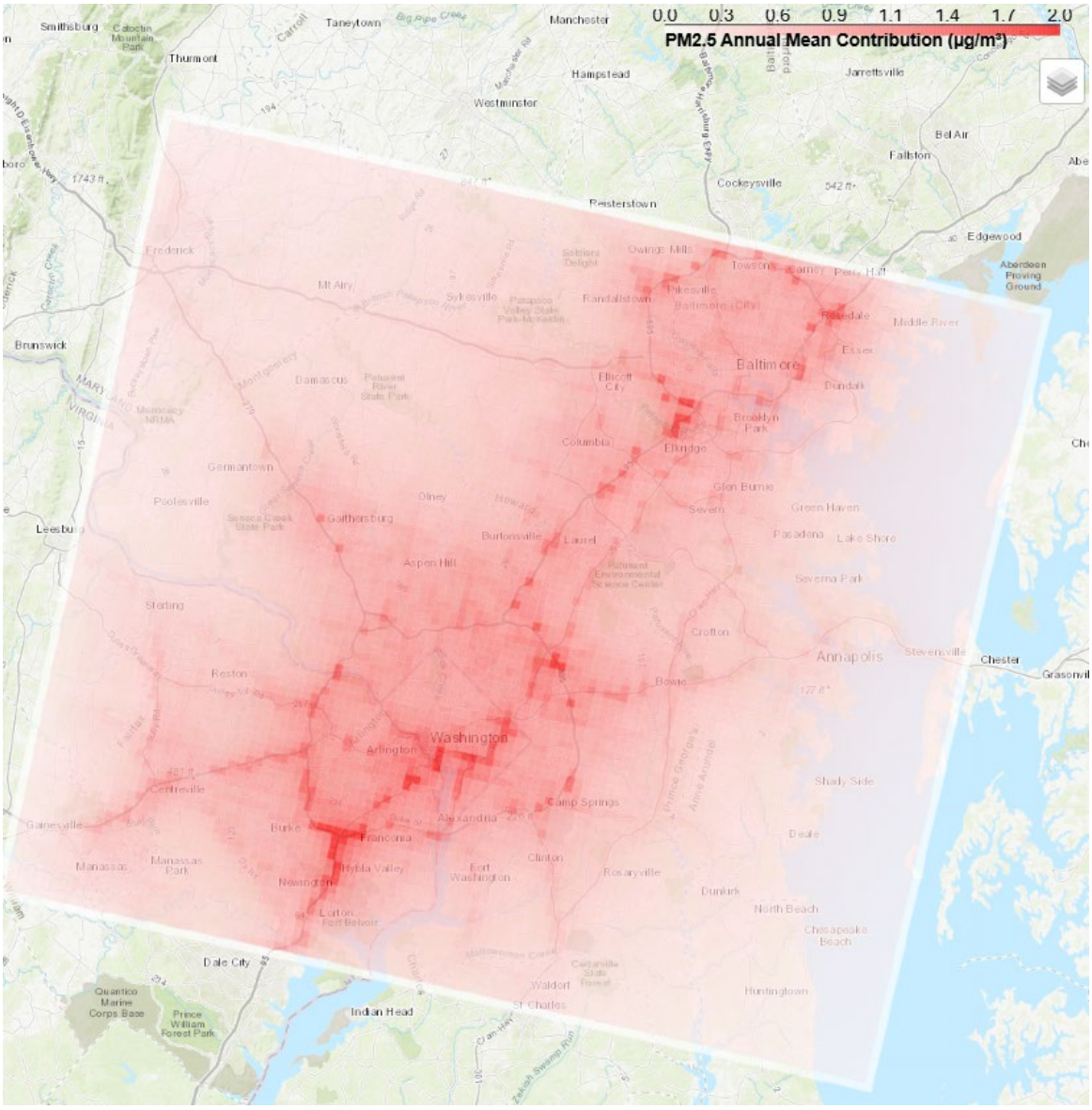

Figure 3-8. CAMx 1 km on-road mobile contribution to 2016 annual average total $PM_{2.5}$ concentrations for Baltimore-Washington domain.

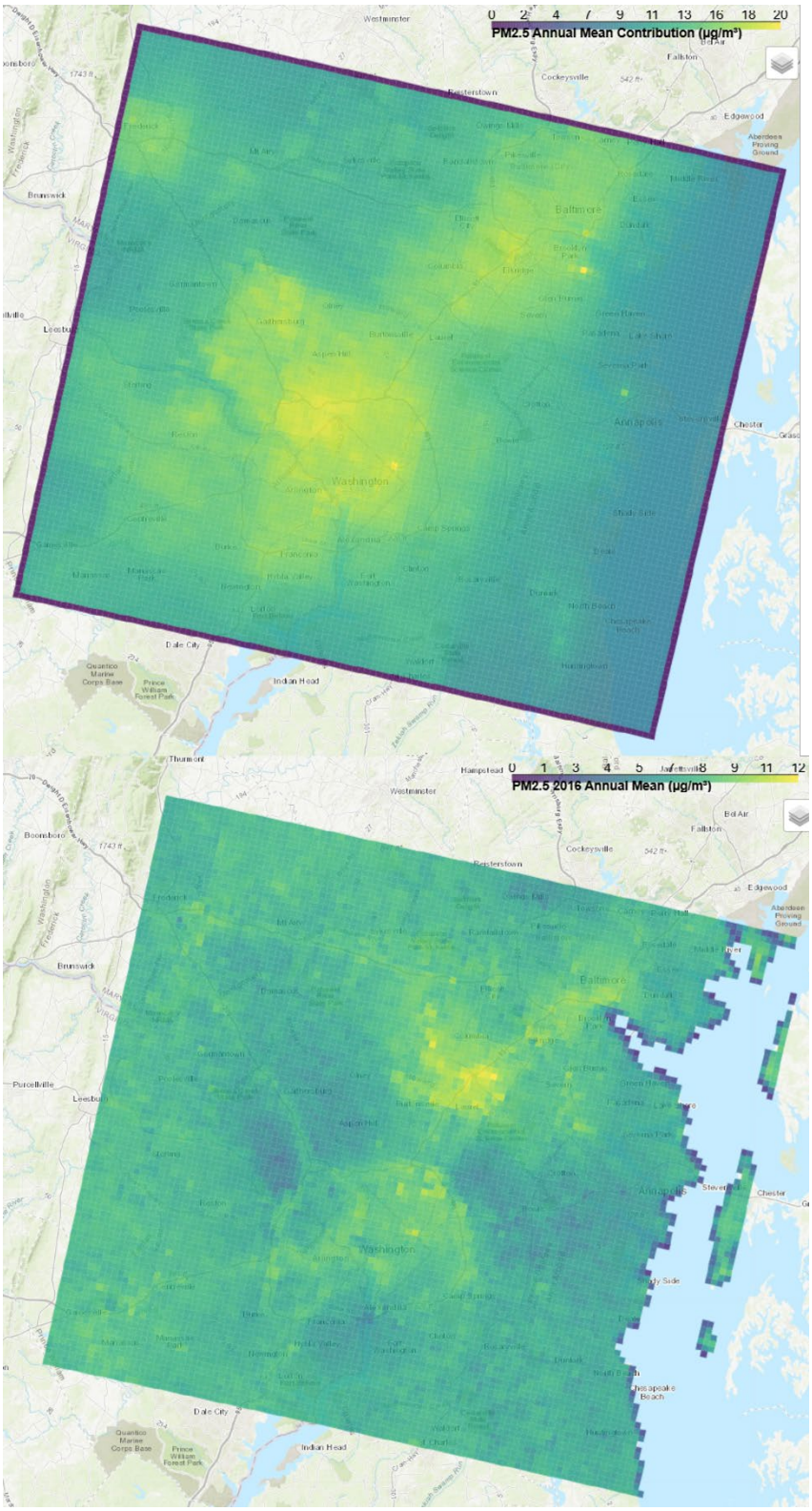

Figure 3-9. 2016 annual average total $PM_{2.5}$ concentrations for Base Case CAMx (top) and $PM_{2.5}$ data product (bottom) for Baltimore-Washington domain.

3.5 Multiple Linear Regression Evaluation

In a recent project sponsored by the Texas Air Quality Research Program (AQRP) focused on NOx emissions in the Houston area, Ramboll and collaborators combined aircraft remote sensing measurements of NO_2 columns with high resolution CAMx simulations (444 m grid) to investigate NOx emissions from individual source-sectors (Goldberg et al., 2024). The CAMx NO_2 columns were biased low compared to both ground-based NO_2 column measurements (20% low) and aircraft-based NO_2 column measurements (31% low) suggesting an underestimate of local NOx emissions. We quantitatively compared source-apportioned CAMx NO_2 columns to the aircraft measurements and used a multiple linear regression (MLR) model to identify on-road, railyard, and "other" NOx emissions as the likeliest cause of this low bias (Figure 3-10). At the same time, NOx emissions from commercial shipping were slightly overestimated. Importantly, we found that several point sources equipped with NOx continuous emission monitors (CEMs) were almost unbiased which supports the validity of the analysis. We modified on-road and shipping NOx emissions in an "optimized NOx" CAMx simulation and increased the background NO_2 which improved agreement with the aircraft data: bias improved from −31% to −10% and r^2 improved from 0.78 to 0.80. This Houston study demonstrates that remote sensing data with fine spatial resolution can be used to improve emission inventories sector-by-sector.

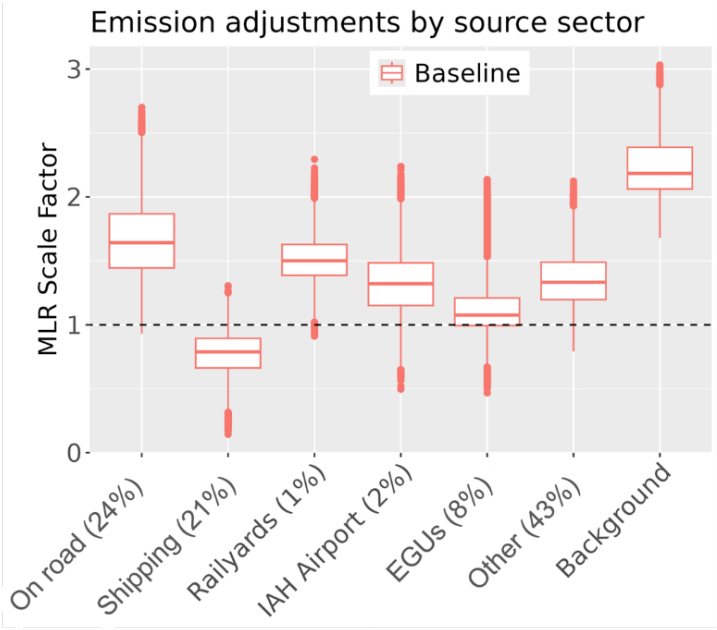

Figure 3-10. NOx emission scale factors by inventory sector derived via Multi Linear Regression (MLR) analysis of NO2 column measurements and baseline CAMx simulations for Houston, TX. Percentages show the fraction of domain-wide NOx emissions from each sector.

Similar to the Houston project, we intended to develop and apply MLR models for each of the three subdomains to investigate whether adjusting on-road emissions and/or the other emissions could improve agreement between modeled $PM_{2.5}$ and the $PM_{2.5}$ data product. As a first step, we developed location-matched daily $PM_{2.5}$ concentrations for the Base Case CAMx simulation and $PM_{2.5}$ data product. We present scatter plots showing 24-hour average $PM_{2.5}$ concentrations for the CAMx Base Case 1 km (y-axis) against the $PM_{2.5}$ data product (x-axis) on both linear (left panel) and log (right panel) scales for all CAMx grid cells in the Phoenix domain in Figure 3-11. Of the three urban areas,

Phoenix had the largest CAMx $PM_{2.5}$ concentrations relative to the data product (see Figure 3-11), which could indicate impacts from dust storms, fires or other emission sources. Because we do not see the same magnitudes in the CAMx scatter plots in Section 3.3, we know that these high PM events are occurring away from monitor locations. Scatter plots for Dallas-Fort Worth (Figure 3-12) and Baltimore-Washington (Figure 3-13) also show some very large CAMx $PM_{2.5}$ concentrations (over 100 µg m^{-3}) where the $PM_{2.5}$ data product is much lower (generally less than 12 µg m^{-3}).

Ultimately, we found that agreement between the $PM_{2.5}$ data product and the CAMx results was not sufficient to perform a meaningful MLR evaluation. Our evaluation in Section 3.3 demonstrated excellent agreement between the $PM_{2.5}$ data product and $PM_{2.5}$ observations at monitor locations. But we lack a methodology to evaluate the $PM_{2.5}$ data product away from monitor locations. Additionally, the data product is itself a model result (i.e. data fusion) rather than a direct observation. Nonetheless, MLR results (example in Figure 3-10) preview what could be done when a TEMPO $PM_{2.5}$ data product is made available operationally.

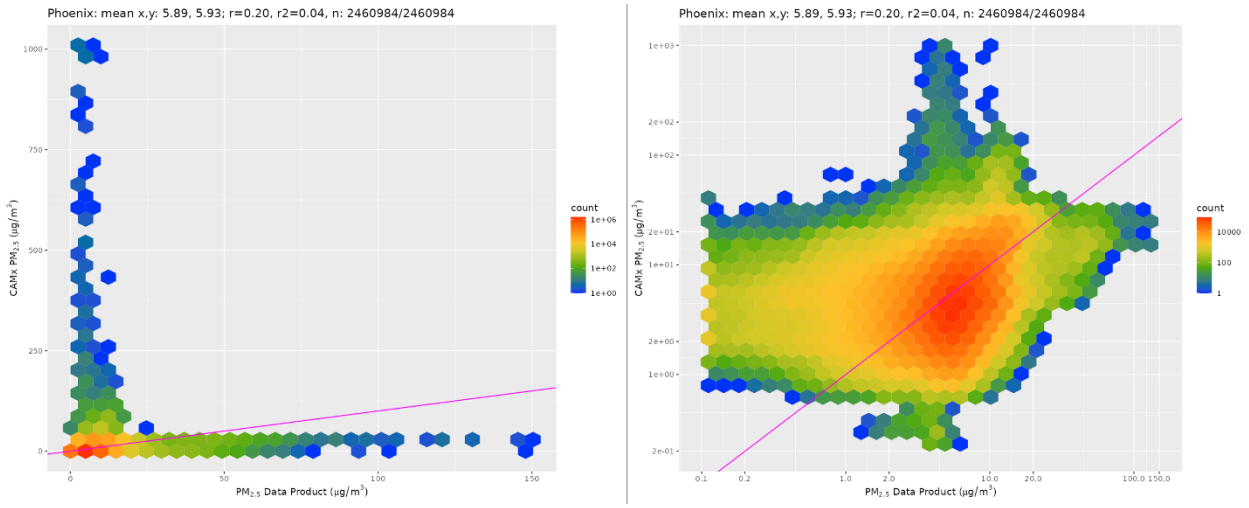

Figure 3-11. Scatter plots showing 24-hour averaged $PM_{2.5}$ concentrations for the Base Case CAMx model against the $PM_{2.5}$ data product on a linear scale (left panel) and log scale (right) for the Phoenix 1 km domain.

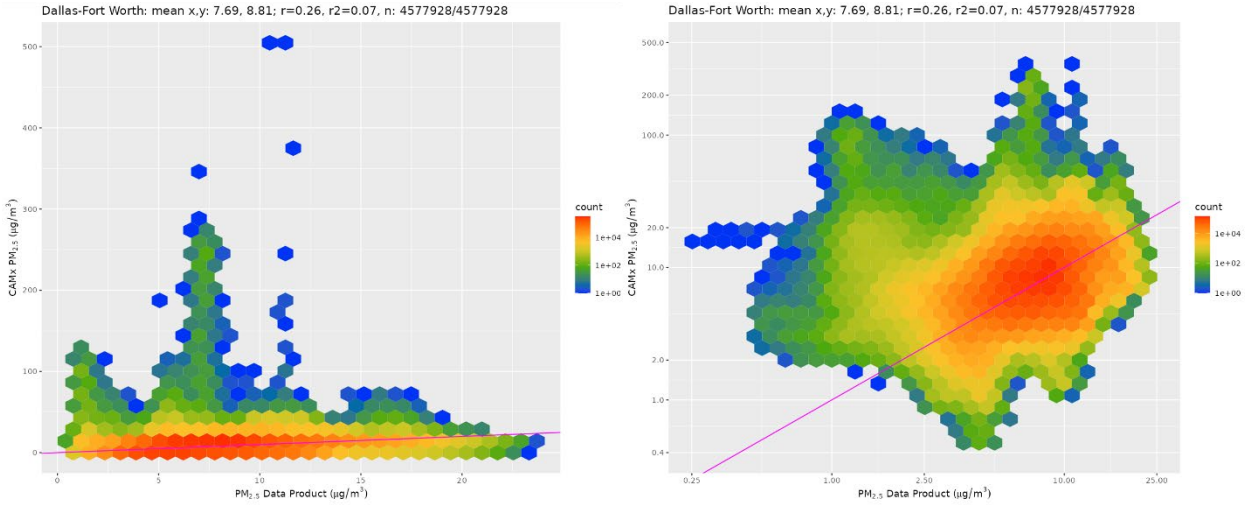

Figure 3-12. Scatter plots showing 24-hour averaged $PM_{2.5}$ concentrations for the Base Case CAMx model against the $PM_{2.5}$ data product on a linear scale (left panel) and log scale (right) for the Dallas-Fort Worth 1 km domain.

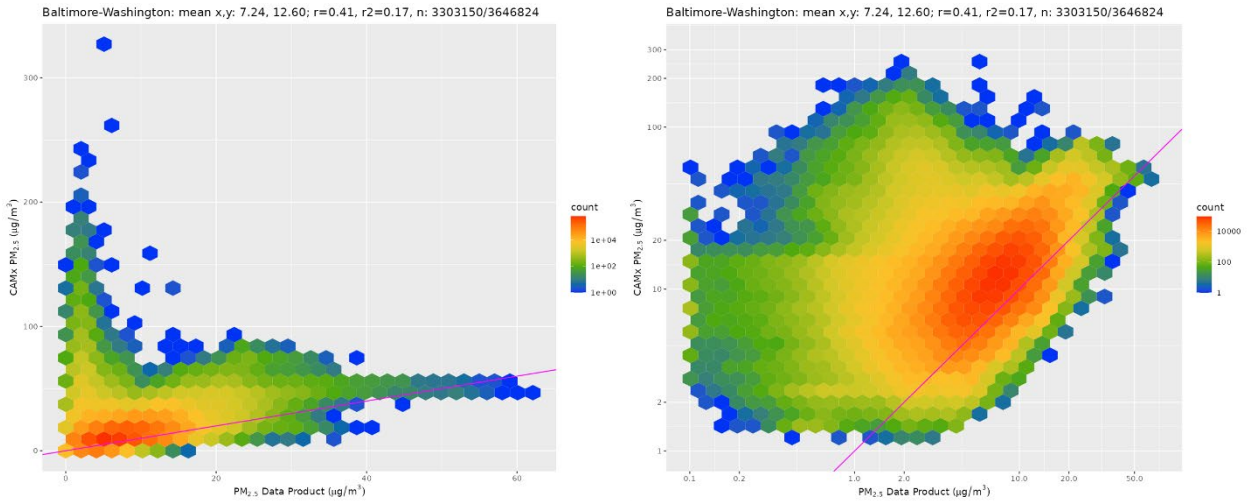

Figure 3-13. Scatter plots showing 24-hour averaged $PM_{2.5}$ concentrations for the Base Case CAMx model against the $PM_{2.5}$ data product on a linear scale (left panel) and log scale (right) for the Baltimore-Washington 1 km domain.

4.0 CONCLUSIONS AND RECOMMENDATIONS

The CRC funded Ramboll to conduct Project A-137 to develop a novel methodology for utilizing satellite data to calibrate fine-grid (1 km) air quality simulations and estimate the source contribution of on-road vehicle emissions to $PM_{2.5}$ ground-level concentrations near highways and transportation corridors.

The TEMPO surface $PM_{2.5}$ product is a promising new source of satellite data that can be used to estimate such $PM_{2.5}$ contributions from on-road vehicles. But as of this writing (August 2025), only one month of preliminary TEMPO surface $PM_{2.5}$ product has been released, and timing of future releases is uncertain. As potential alternative to TEMPO, we investigated AOD column data from GOES and VIIRS, but both have limitations (primarily low data completeness and interference from clouds and reflective surfaces) that prevent their use in this study.

Di et al. (2019) employed an ensemble-based model to estimate date-specific $PM_{2.5}$ concentrations across the contiguous United States at high spatial resolution. The main data sources include MODIS AOD satellite data, OMI satellite NO_2 columns, total and speciated $PM_{2.5}$ surface measurements, CMAQ model concentrations, and MERRA2 modeled total and speciated $PM_{2.5}$ concentrations. The model predicts daily $PM_{2.5}$ concentrations at a resolution of 1 km x 1 km grid cells.

The most recent available data from this "$PM_{2.5}$ data product" is for calendar year 2016, which matches an available CMAQ/CAMx modeling year from EPA with 12 km grid resolution. We therefore developed a new modeling platform based on EPA's 2016 platform with spatially refined on-road mobile emissions for specific metropolitan areas to evaluate against the $PM_{2.5}$ data product.

We developed three CAMx 1 km domains that contain the urban areas of Phoenix, Dallas-Fort Worth and Baltimore-Washington. We selected these cities because they all have major highways and transportation corridors. Our $PM_{2.5}$ model performance evaluation compared our Base Case 1 km CAMx simulations, EPA's 12 km model results, and the $PM_{2.5}$ data product against available 24-hour $PM_{2.5}$ observations within each of the 3 urban areas. In all 3 domains, we found that our Base Case 1 km CAMx simulations increased $PM_{2.5}$ concentrations relative to the EPA 12 km simulations. For Phoenix, this increase was beneficial, as the EPA 12 km simulation underestimated $PM_{2.5}$ concentrations. However, the EPA 12 km simulations for Dallas-Fort Worth and Baltimore-Washington overestimated $PM_{2.5}$, so our Base Case 1 km CAMx simulations exacerbated these positive biases. For all 3 urban areas, the $PM_{2.5}$ data product showed excellent agreement with observations, meeting the Goal criteria (Emery et al., 2017) for bias and error in each area.

Examining the CAMx 1 km on-road vehicle contribution to annual $PM_{2.5}$, we found hotspots that aligned with the transportation networks, but in most cases, were somewhat spotty and did not show consistent enhancements along the entire roadway lengths. These contributions were somewhat small (less than 2 $\mu g\ m^{-3}$) compared to the annual total $PM_{2.5}$ concentrations (8-20 $\mu g\ m^{-3}$ in some locations). The spatial comparison of annual total $PM_{2.5}$ between CAMx and the $PM_{2.5}$ data product was also somewhat poor. The CAMx $PM_{2.5}$ concentrations tended to be higher overall, and hotspots generally did not match up well between the two products. Neither of the two total $PM_{2.5}$ sets of maps showed much roadway network signal, other than in West Phoenix, where other emission sectors are contributing.

Due to poor agreement between the CAMx simulation and the $PM_{2.5}$ data product, we were not able to gain useful information about emissions from MLR models developed for the three cities. The limitations of the modeling (12 km resolution for meteorology and most emission sectors, simple

spatial interpolation technique applied to on-road and railway emissions, etc.) in this study likely play some role in the poor agreement between the CAMx results and the $PM_{2.5}$ data product.

While the $PM_{2.5}$ data product showed excellent agreement with $PM_{2.5}$ concentrations at monitor locations, we lack a methodology to evaluate the $PM_{2.5}$ data product away from monitor locations. Additionally, the data product is itself a model result (i.e. data fusion) rather than a direct observation. Nonetheless, MLR models could be deployed when a TEMPO or other suitable $PM_{2.5}$ satellite product is made available.

We recommend the following for future work:

- Develop and evaluate a new CAMx modeling platform that uses high resolution meteorological simulations over one or more urban areas and "bottom-up" emissions processing at high resolution for on-road mobile and other sectors
- Develop new MLR models that evaluate $PM_{2.5}$ emissions from the new high-resolution CAMx simulations using TEMPO or another suitable satellite-based $PM_{2.5}$ product as they become available

5.0 REFERENCES

Boylan, J. W. and A. G. Russell. 2006. PM and light extinction model performance metrics, goals, and criteria for three-dimensional air quality models. *Atmos. Env.* Vol. 40, Issue 26, pp. 4946-4959. August. (https://www.sciencedirect.com/science/article/pii/S1352231006000690).

Colella, P., and P.R. Woodward. 1984. The Piecewise Parabolic Method (PPM) for Gas-dynamical Simulations. J. Comp. Phys., 54, 174-201.

Di, Q., Amini, H., Shi, L., Kloog, I., Silvern, R., Kelly, J., Sabath, M.B., Choirat, C., Koutrakis, P., Lyapustin, A. and Wang, Y., 2019. An ensemble-based model of $PM_{2.5}$ concentration across the contiguous United States with high spatiotemporal resolution. Environment International, 130, p.104909.

Emery, C., Liu, Z., Russell, A.G., Odman, M.T., Yarwood, G. and Kumar, N., 2017. Recommendations on statistics and benchmarks to assess photochemical model performance. *Journal of the Air & Waste Management Association*, *67*(5), pp.582-598.

EPA. 2019. Meteorological Model Performance for Annual 2016 Simulation WRF v3.8. U.S. Environmental Protection Agency, Office of Air Quality Planning and Standards, Air Quality Assessment Division, Research Triangle Park, NC. EPA-454/R-19-010. https://www.epa.gov/sites/default/files/2020-10/documents/met_model_performance-2016_wrf.pdf

Eyth, A., Vukovich, J., Farkas, C., Godfrey, J., & Seltzer, K. 2023. Technical Support Document (TSD): Preparation of Emissions Inventories for the 2016v3 North American Emissions Modeling Platform. US Environmental Protection Agency, Office of Air Quality Planning and Standards, Air Quality Assessment Division. https://www.epa.gov/system/files/documents/2023-03/2016v3_EmisMod_TSD_January2023_1.pdf

Fu, D., Gueymard, C.A. and Xia, X., 2023. Validation of the improved GOES-16 aerosol optical depth product over North America. Atmospheric Environment, 298, p.119642.

Goldberg, D., de Foy, B., Nawaz, M.O., Johnson, J., Yarwood, G., Judd L., 2024. Quantifying NOx Emission Sources in Houston, Texas using Remote Sensing Aircraft Measurements and Source Apportionment Regression Models. Submitted for publication in ES&T Air.

Homer, C., Dewitz, J., Yang, L., Jin, S., Danielson, P., Xian, G., Coulston, J., Herold, N., Wickham, J. and Megown, K., 2015. Completion of the 2011 National Land Cover Database for the conterminous United States–representing a decade of land cover change information. Photogrammetric Engineering & Remote Sensing, 81(5), pp.345-354.

Ran, L., Gilliam, R., Binkowski, F. S., Xiu, A., Pleim, J., & Band, L. (2015). Sensitivity of the Weather Research and Forecast/Community Multiscale Air Quality modeling system to MODIS LAI, FPAR, and albedo. Journal of Geophysical Research: Atmospheres, 120(16), 8491-8511.

Simon, H., K. Baker and S. Phillips. 2012. Compilations and Interpretation of Photochemical Model Performance Statistics Published between 2006 and 2012. *Atmos. Env.* 61 (2012) 124-139. December. (http://www.sciencedirect.com/science/article/pii/S135223101200684X).

Zhang, L., S. Gong, J. Padro, L. Barrie. 2001. A size-segregated particle dry deposition scheme for an atmospheric aerosol module. Atmos. Environ., 35, 549-560.

Zhang, L., J. R. Brook, and R. Vet. 2003. A revised parameterization for gaseous dry deposition in air-quality models. Atmos. Chem. Phys., 3, 2067–2082.